Mott Transition and Suppression of Orbital Fluctuations in Orthorhombic $3d^1$ Perovskites

E. Pavarini,[1] S. Biermann,[2] A. Poteryaev,[3] A. I. Lichtenstein,[3] A. Georges,[2] and O. K. Andersen[4]

[1]*INFM and Dipartimento di Fisica "A. Volta," Università di Pavia, Via Bassi 6, I-27100 Pavia, Italy*
[2]*Centre de Physique Théorique, Ecole Polytechnique, 91128 Palaiseau Cedex, France*
[3]*NSRIM, University of Nijmegen, NL-6525 ED Nijmegen, The Netherlands*
[4]*Max-Planck-Institut für Festkörperforschung, Heisenbergstrasse 1, D-70569 Stuttgart, Germany*

(Received 4 September 2003; published 30 April 2004)

Using t_{2g} Wannier functions, a low-energy Hamiltonian is derived for orthorhombic $3d^1$ transition-metal oxides. Electronic correlations are treated with a new implementation of dynamical mean-field theory for noncubic systems. Good agreement with photoemission data is obtained. The interplay of correlation effects and cation covalency ($GdFeO_3$-type distortions) is found to suppress orbital fluctuations in $LaTiO_3$ and even more in $YTiO_3$, and to favor the transition to the insulating state.

DOI: 10.1103/PhysRevLett.92.176403 PACS numbers: 71.30.+h, 71.15.Ap, 71.27.+a

Transition-metal perovskites have attracted much interest because of their unusual electronic and magnetic properties arising from narrow $3d$ bands and strong Coulomb correlations [1]. The $3d^1$ perovskites are particularly interesting, since seemingly similar materials have very different electronic properties: $SrVO_3$ and $CaVO_3$ are correlated metals with mass enhancements of, respectively, 2.7 and 3.6 [2], while $LaTiO_3$ and $YTiO_3$ are Mott insulators with gaps of, respectively, 0.2 and 1 eV [3].

In the Mott-Hubbard picture the metal-insulator transition occurs when the ratio of the on-site Coulomb repulsion to the one-electron bandwidth exceeds a critical value U_c/W, which increases with orbital degeneracy [4,5]. In the ABO_3 perovskites the transition-metal ions (B) are on a nearly cubic (orthorhombic) lattice and at the centers of corner-sharing O_6 octahedra. The $3d$ band splits into $pd\pi$-coupled t_{2g} bands and $pd\sigma$-coupled e_g bands, of which the former lie lower, have less O character and couple less to the octahedra than the latter. The simplest theories for the d^1 perovskites [1] are therefore based on a Hubbard model with three *degenerate*, $\frac{1}{6}$-filled t_{2g} bands per B ion, and the variation of the electronic properties along the series is ascribed to a progressive reduction of W due to the increased bending of the $pd\pi$ hopping paths (BOB bonds).

This may not be the full explanation of the Mott transition however, because a splitting of the t_{2g} levels can effectively lower the degeneracy. In the correlated metal, the relevant energy scale is the reduced bandwidth associated with quasiparticle excitations. Close to the transition, this scale is of order $\sim ZW$, with $Z \sim 1 - U/U_c$, and hence much smaller than the original bandwidth W. A level splitting by merely ZW is sufficient to lower the effective degeneracy all the way from a threefold to a nondegenerate single band [6]. This makes the insulating state more favorable by reducing U_c/W [5,6]. Unlike the e_g-band perovskites, such as $LaMnO_3$, where large (10%) cooperative Jahn-Teller (JT) distortions of the octahedra indicate that the orbitals are spatially ordered, in the t_{2g}-band perovskites the octahedra are almost perfect. The t_{2g} orbitals have therefore often been assumed to be degenerate. If that is true, it is conceivable that quantum fluctuations lead to an orbital *liquid* [7] rather than orbital ordering. An important experimental constraint on the nature of the orbital physics is the observation of an isotropic, small-gap spin-wave spectrum in both insulators [8]. This is remarkable because $LaTiO_3$ is a G-type antiferromagnet with $T_N = 140$ K, $m = 0.45\mu_B$, and a 3% JT stretching along **a** [9], while $YTiO_3$ is a ferromagnet with $T_C = 30$ K, $m_0 \sim 0.8\mu_B$, and a 3% stretching along **y** on sites 1 and 3, and **x** on 2 and 4 [10] (see Fig. 1).

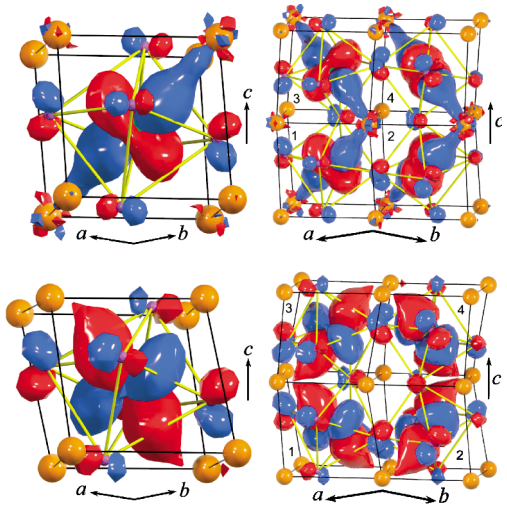

FIG. 1 (color). *Pbnm* primitive cells (right panels), subcells 1 (left panels), and the occupied t_{2g} orbitals for $LaTiO_3$ (top panels) and $YTiO_3$ (bottom panels) according to the LDA + DMFT calculation. The oxygens are violet, the octahedra yellow, and the cations orange. In the global, cubic xyz system directed approximately along the Ti-O bonds, the orthorhombic translations are $\mathbf{a}=(1,-1,0)(1+\alpha)$, $\mathbf{b}=(1,1,0)(1+\beta)$, and $\mathbf{c}=(0,0,2)(1+\gamma)$, with α, β, and γ small. The Ti sites 1 to 4 are $\mathbf{a}/2$, $\mathbf{b}/2$, $(\mathbf{a}+\mathbf{c})/2$, and $(\mathbf{b}+\mathbf{c})/2$. The La(Y) ab plane is a mirror ($z \leftrightarrow -z$) and so is the Ti bc plane ($x \leftrightarrow y$) when combined with the translation $(\mathbf{b}-\mathbf{a})/2$.

We shall find that the t_{2g} degeneracy *is lifted* at the classical level. This is not due to the small JT distortions via OB $pd\pi$ coupling, but to the $GdFeO_3$-type distortion which tilts the corner-sharing octahedra around the b axis (by 0°, 9°, 12°, and 20°) and rotates them around the c axis (by 0°, 7°, 9°, and 13°), as we progress from cubic $SrVO_3$ via $CaVO_3$ and $LaTiO_3$ to $YTiO_3$ [9–12]. This distortion is driven by the increasing oxygen-cation (OA) $pd\sigma$ covalency, and it primarily pulls closer four of the 12 oxygens neighboring a given cation [13]. Moreover, two to four of the eight cations neighboring a given B ion are pulled closer [14]. The t_{2g} orbitals couple to the OA distortion via oxygen (BOA $dp\pi$-$pd\sigma$), and they couple directly (AB $dd\sigma$) to the AB distortion. As seen in Fig. 1, the orthorhombic $GdFeO_3$-type distortion also leads to quadrupling of the cell. These findings are consistent with conclusions drawn in the most recent model Hartree-Fock study [15]. The correct magnetic orders in $LaTiO_3$ and $YTiO_3$ were also obtained with the LDA + U method [16]. The predicted moment and orbital order in $YTiO_3$ were confirmed by NMR [17] and neutron scattering [18], but not in $LaTiO_3$. These static mean-field methods are not appropriate for the metallic systems, however.

In this Letter, we shall (i) present a new implementation of a many-body method [19,20], which allows for a quantitative, material-specific description of *both* the Mott transition and the orbital physics, and (ii) use it to explain why some of the d^1 perovskites are metallic and others are insulators, why the metals have different mass enhancements and the insulators different gaps. Such properties can be described by a low-energy, multiband Hubbard Hamiltonian,

$$H = H^{\mathrm{LDA}} + \frac{1}{2}\sum_{imm'\sigma} U_{mm'} n_{im\sigma} n_{im'-\sigma} + \frac{1}{2}\sum_{im(\neq m')\sigma} (U_{mm'} - J_{mm'}) n_{im\sigma} n_{im'\sigma}, \qquad (1)$$

where $n_{im\sigma} = a^{+}_{im\sigma} a_{im\sigma}$, and $a^{+}_{im\sigma}$ creates an electron with spin σ in a localized orbital m at site i. This Hamiltonian depends on how the $im\sigma$ orbitals are chosen. H^{LDA} is the one-electron part given by density-functional theory [LDA (local-density approximation)], which should provide the proper material dependence. Recently it has become feasible to solve (1) using the *dynamical* mean-field theory (DMFT) [19] and to obtain realistic physical properties [20]. In the original LDA + DMFT implementations it was assumed that the on-site block(s) of the single-particle Green function is diagonal in the space of the correlated orbitals, and these were taken as orthonormal linear muffin-tin orbitals (LMTOs) *approximated* by truncated and renormalized partial waves.

Although these approximations are good for cubic t_{2g} systems such as $SrVO_3$ [21], they deteriorate with the degree of distortion. Our new implementation of LDA + DMFT uses a set of localized Wannier functions in order to construct a realistic Hamiltonian (1), which is then solved by DMFT, including the nondiagonal part of the on-site self-energy.

For an isolated set of bands, a set of Wannier functions constitutes a *complete*, orthonormal set of orbitals with *one* orbital per band. For the d^1 perovskites we take the correlated orbitals to be three localized t_{2g} Wannier orbitals, and in H^{LDA} we neglect the degrees of freedom from all other bands. In order to be complete, such a Wannier orbital must have a tail with, e.g., O $p\pi$ and A d characters. Our Wannier orbitals are symmetrically orthonormalized Nth-order muffin-tin orbitals (NMTOs) [22], which have all partial waves other than B xy, yz, and zx downfolded. Such a t_{2g} NMTO can have on-site e_g character and that allows the orbital to orient itself after the surroundings, although xy, yz, and zx refers to the global cubic axes defined in Fig. 1. Fourier transformation of the orthonormalized 12×12 NMTO Hamiltonian, $H^{\mathrm{LDA}}(\mathbf{k})$, yields on-site blocks and hopping integrals. For the on-site Coulomb interactions in Eq. (1), we use the common assumption that, as in the isotropic case, they can be expressed in terms of two parameters: $U_{mm} = U$, $U_{mm'} = U - 2J$, and $J_{mm'(\neq m)} = J$ [23]. From Ref. [24], $J =$ 0.68 eV for the vanadates and 0.64 eV for the titanates. Since our Hamiltonian involves only correlated orbitals, so that the number of correlated electrons is fixed, the double-counting correction amounts to an irrelevant shift of the chemical potential. H is now solved within DMFT, i.e., under the assumption that the components of the self-energy between different sites can be neglected. As a result, the self-energy can be obtained from the solution of an effective local impurity model which involves only three correlated orbitals. In contrast to all previous studies, we take all components of the self-energy matrix $\Sigma_{mm'}$ between different Wannier functions on a given B site into account [25]. From this 3×3 matrix, by use of the $Pbnm$ symmetry (Fig. 1), we construct a 12×12 block-diagonal self-energy matrix. The latter is then used together with $H^{\mathrm{LDA}}(\mathbf{k})$ to obtain the Green function at a given $\mathbf{k}$ point. Fourier transformation over the entire Brillouin zone yields the local Green function associated with a primitive cell, and its 3×3 on-site block is used in the DMFT self-consistency condition in the usual manner. The 3-orbital impurity problem is solved by a numerically exact quantum Monte Carlo (QMC) scheme [26]. To access temperatures down to 770 K, we use up to 100 slices in imaginary time. 10^6 QMC sweeps and 15–20 DMFT iterations suffice to reach convergence. Finally, the spectral function is obtained using the maximum entropy method [27].

We now present the LDA results for the four perovskites. Figure 2 displays the on-site density of states (DOS) matrix $N_{mm'}(\varepsilon)$ in the representation of the xy, yz, and zx Wannier functions. $SrVO_3$ is cubic and its t_{2g} band with a width $W = 2.8$ eV consists of three noninteracting subbands, each of which is nearly 2D and gives rise to a nearly logarithmic DOS peak. In $CaVO_3$,

W is reduced to 2.4 eV because the Wannier orbitals are misaligned by the $GdFeO_3$-type distortion and because some of their O $2p$ character is stolen by the increased OA covalency, which drives this distortion. The energy of the xy Wannier orbital (the center of gravity of $N_{xy,xy}$) is 80 meV lower than that of the degenerate xz and yz orbitals, and small off-diagonal DOS elements appear. Going from the vanadates to the titanates, the effects of OA and (Ad) (Bt_{2g}) covalency increase dramatically, because now A and B are 1st- rather than 3rd-nearest neighbors in the periodic table. As a consequence, the increased misalignment and loss of oxygen character reduce the bandwidths to 2.1 and 2.0 eV in $LaTiO_3$ and $YTiO_3$, and weak hybridization with the A d bands deforms the t_{2g} band. A pseudogap which starts out as a splitting of the van Hove peak in $CaVO_3$ deepens and moves to lower occupancy as we progress to $LaTiO_3$ and $YTiO_3$. The deep pseudogap in $YTiO_3$ is mainly caused by the hybridization with the Y xy orbital. The xy, yz, and zx Wannier orbitals are now strongly mixed and diagonalization of the on-site blocks of H^{LDA} yields three singly degenerate levels with the middle (highest) being 140 (200) meV above the lowest in $LaTiO_3$ and 200 (330) meV in $YTiO_3$. This splitting is not only an order of magnitude smaller than the t_{2g} bandwidth, but also smaller than the subband widths, in particular, for $LaTiO_3$. As a consequence, the eigenfunction for the lowest level is occupied by merely 0.45 electron in $LaTiO_3$ and 0.50 in $YTiO_3$, while the remaining 0.55 (0.50) electron occupies the two other eigenfunctions. The eigenfunction on site 1 with the lowest energy is $0.604|xy\rangle + 0.353|xz\rangle + 0.714|yz\rangle$ in $LaTiO_3$ and $0.619|xy\rangle - 0.073|xz\rangle + 0.782|yz\rangle$ in $YTiO_3$. The splittings are large compared with the spin-orbit splitting (20 meV) and kT, and they are not caused by the JT distortions, as we have verified by turning them off in the calculations.

Next, we turn to the LDA + DMFT results. Calculations were performed for several values of U between 3 and 6 eV. We found that the critical ratio U_c/W decreases when going along the series: $SrVO_3$, $CaVO_3$, $LaTiO_3$, and $YTiO_3$. This is consistent with the increasing splitting of the t_{2g} levels and indicates that the Mott transition in the d^1 series is driven as much by the decrease of effective degeneracy as by the reduction of the bandwidth. The main features of the photoemission spectra for all four materials, as well as the correct values of the Mott-Hubbard gap for the insulators [3], are reproduced by taking U constant $\sim$5 eV. This is satisfying because U is expected to be similar for vanadates and titanates, although slightly smaller for the latter [24]. In Fig. 3 we show the DMFT spectral functions together with the LDA total DOS. For cubic $SrVO_3$ we reproduce the results of previous calculations [21,28]: the lower Hubbard band (LHB) is around -1.8 eV and the upper Hubbard band (UHB) around 3 eV. Going to $CaVO_3$, the quasiparticle peak loses weight to the LHB which remains at -1.8 eV while the UHB moves down to 2.5 eV. These results are in good agreement with photoemission data [29] and show that $SrVO_3$ and $CaVO_3$ are rather similar, with the latter slightly more correlated. Similar conclusions were drawn in Ref. [21]. From the linear regime of the self-energy at small Matsubara frequencies we estimate the quasiparticle weight to be $Z = 0.45$ for $SrVO_3$ and 0.29 for $CaVO_3$. For a $\mathbf{k}$-independent self-energy, as assumed in DMFT, this yields $m^*/m = 1/Z = 2.2$ for $SrVO_3$ and 3.5 for $CaVO_3$, in reasonable agreement with the optical conductivity values 2.7 and 3.6 [2].

For $LaTiO_3$ and $YTiO_3$ the LHB is around -1.5 eV, in accord with photoemission [30]. Despite very similar bandwidths, the gaps are very different, 0.3 and 1 eV, and this also agrees with experiments [3]. This is consistent with our findings that the t_{2g}-level splittings are smaller and U_c/W is larger in $LaTiO_3$ than in $YTiO_3$ where the orbital degeneracy is effectively 1. Diagonalization of the matrix of occupation numbers reveals that for the titanates *one orbital per site is nearly full*, in contrast to LDA. It contains 0.88 electron in $LaTiO_3$ and 0.96 in $YTiO_3$. The orbital polarization increases

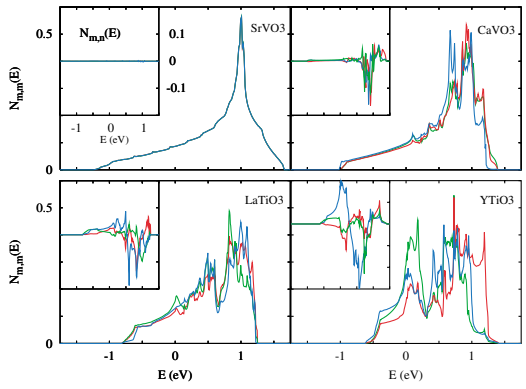

FIG. 2 (color). t_{2g} LDA DOS matrix (states/eV/spin/band) in the Wannier representation. On-site-1 elements: $N_{xz,xz}$ (red) $N_{yz,yz}$ (green), and $N_{xy,xy}$ (blue). Insets: $N_{yz,xz}$ (red), $N_{xz,xy}$ (green), and $N_{xy,yz}$ (blue). $\varepsilon_F \equiv 0$.

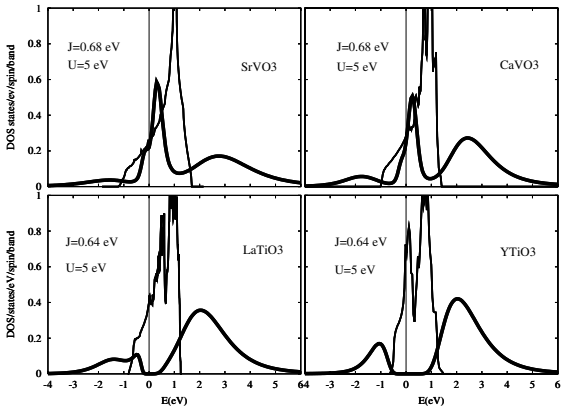

FIG. 3. DMFT spectral function at $T = 770$ K (thick line) and LDA DOS (thin line). $\mu \equiv 0$.

around the metal-insulator transition and becomes complete thereafter. Thus, for the vanadates, each orbital is approximately 1/3 occupied for all U in the range 0 to 6 eV. The *nearly complete* orbital polarization found by LDA + DMFT for the two insulators indicates that correlation effects in the paramagnetic Mott insulating state considerably decrease orbital fluctuations and makes it unlikely that $YTiO_3$ is a realization of an orbital liquid [7]. In $LaTiO_3$ some orbital fluctuations are still active, although quite weak. The occupied orbital in LDA + DMFT is $0.586|xy\rangle + 0.275|xz\rangle + 0.762|yz\rangle$ for $LaTiO_3$ and $0.622|xy\rangle - 0.029|xz\rangle + 0.782|yz\rangle$ for $YTiO_3$. Hence, it is nearly identical with the ones we obtained from the LDA as having the lowest energy. For $YTiO_3$ our orbital is similar to the one obtained in Ref. [16] and for $LaTiO_3$ it is similar to the one obtained in Refs. [9,15]. Our accurate Wannier functions show *why* these orbitals (Fig. 1, left panels) have the lowest energy: The positive (blue) lobes have bonding $3z_{111}^2 - 1 = (|xy\rangle + |xz\rangle + |yz\rangle)/\sqrt{3}$ character on the nearest cations—those along [111]—and the negative (red) lobes have bonding xy character on the next-nearest cations—those along [1–11]—whose oxygen surrounding is favorable for this type of bond, i.e., where (Op) (Yxy) $pd\sigma$ hybridization is strong. The former type of AB covalency dominates in $LaTiO_3$, while the latter dominates in $YTiO_3$, where the shortest YO bond is merely 10% longer than the TiO bond. The difference seen (Fig. 1, right panels) between the orbital orders in the two compounds is therefore quantitative rather than qualitative; it merely reflects the extent to which the orbital has the bc plane as a mirror. The two different JT distortions of the oxygen square are reactions to, rather than the causes of the difference in the orbital orders. This difference is reflected in the hopping integrals between nearest neighbors: $t_x = t_y = 99$ (38) meV and $t_z = 105$ (48) meV for $LaTiO_3$ ($YTiO_3$). These hoppings are fairly isotropic and twice larger in $LaTiO_3$ than in $YTiO_3$. Moreover, the hoppings to the two excited orbitals are stronger in $YTiO_3$ than in $LaTiO_3$. All of this is consistent with $LaTiO_3$ being G-type anti- and $YTiO_3$ ferromagnetic at low temperature, and it warrants detailed future calculations of the spin-wave spectra.

In conclusion, we have extended the LDA + DMFT approach to the noncubic case using *ab initio* downfolding in order to obtain a low-energy Wannier Hamiltonian. Applying this method to the Mott transition in $3d^1$ perovskites, we have explained the photoemission spectra and the values of the Mott gap without adjustable parameters, except a single value of U. The Mott transition is driven by correlation effects and $GdFeO_3$-type distortion through reduction, not only of bandwidth, but also of effective orbital degeneracy. Correlation effects and cation covalency suppress orbital fluctuations in the high-temperature paramagnetic insulating phase of $LaTiO_3$ and $YTiO_3$.

We thank J. Nuss, G. Khaliullin, E. Koch, J. Merino, M. Rozenberg, A. Bringer, and M. Imada for useful discussions and the KITP Santa Barbara for hospitality and support (NSF Grant No. PHY99-07949). Calculations were performed at MPI-FKF Stuttgart and IDRIS Orsay (Project No. 021393). S. B. acknowledges support from the CNRS and the EU (Contract No. HPMF-CT-2000-00658).

[1] M. Imada, A. Fujimori, and Y. Tokura, Rev. Mod. Phys. **70**, 1039 (1998).
[2] H. Makino *et al.*, Phys. Rev. B **58**, 4384 (1998).
[3] Y. Okimoto *et al.*, Phys. Rev. B **51**, 9581 (1995).
[4] M. J. Rozenberg, Phys. Rev. B **55**, R4855 (1997).
[5] E. Koch, O. Gunnarsson, and R. M. Martin, Phys. Rev. B **60**, 15 714 (1999); S. Florens *et al.*, *ibid.* **66**, 205102 (2002).
[6] N. Manini, G. E. Santoro, A. Dal Corso, and E. Tosatti, Phys. Rev. B **66**, 115107 (2002).
[7] G. Khaliullin and S. Maekawa, Phys. Rev. Lett. **85**, 3950 (2000).
[8] B. Keimer *et al.*, Phys. Rev. Lett. **85**, 3946 (2000); C. Ulrich *et al.*, Phys. Rev. Lett. **89**, 167202 (2002).
[9] M. Cwik *et al.*, Phys. Rev. B **68**, 060401 (2003).
[10] M. Eitel *et al.*, J. Less-Common Met. **116**, 95 (1986).
[11] M. J. Rey *et al.*, J. Solid State Chem. **86**, 101 (1990).
[12] M. H. Jung and H. Nakotte (unpublished).
[13] By 0%, 10%, 13%, and 21% of the average OA distance.
[14] By 0%, 3%, 4%, and 10% of the average AB distance.
[15] M. Mochizuki and M. Imada, Phys. Rev. Lett. **91**, 167203 (2003); T. Mizokawa, D. I. Khomskii, and G. A. Sawatzky, Phys. Rev. B **60**, 7309 (1999).
[16] I. Solovyev, N. Hamada, and K. Terakura, Phys. Rev. B **53**, 7158 (1996); H. Sawada and K. Terakura, *ibid.* **58**, 6831 (1998).
[17] M. Itoh *et al.*, J. Phys. Soc. Jpn. **68**, 2783 (1999).
[18] J. Akimitsu *et al.* J. Phys. Soc. Jpn. **70**, 3475 (2001).
[19] A. Georges, G. Kotliar, W. Kraut, and M. J. Rozenberg, Rev. Mod. Phys. **68**, 13 (1996).
[20] V. Anisimov *et al.*, J. Phys. Condens. Matter **9**, 7359 (1997); A. I. Lichtenstein and M. I. Katsnelson, Phys. Rev. B **57**, 6884 (1998).
[21] I. A. Nekrasov *et al.*, cond-mat/0211508.
[22] O. K. Andersen and T. Saha-Dasgupta, Phys. Rev. B **62**, 16 219 (2000); Bull. Mater. Sci. **26**, 19 (2003).
[23] R. Fresard and G. Kotliar, Phys. Rev. B **56**, 12 909 (1997).
[24] T. Mizokawa and A. Fujimori, Phys. Rev. B **54**, 5368 (1996).
[25] $\Sigma_{mm'(\neq m)}(\omega) \neq 0$ in noncubic systems, also in the eigenrepresentation of the density matrix. In Fig. 2, a large $N_{mm'(\neq m)}$ points to a large $\Sigma_{mm'(\neq m)}$.
[26] J. E. Hirsch and R. M. Fye, Phys. Rev. Lett. **56**, 2521 (1986).
[27] J. E. Gubernatis, M. Jarrell, R. N. Silver, and D. S. Sivia, Phys. Rev. B **44**, 6011 (1991).
[28] A. Liebsch, Phys. Rev. Lett. **90**, 096401 (2003).
[29] K. Maiti *et al.*, Europhys. Lett. **55**, 246 (2001); A. Sekiyama *et al.*, cond-mat/0206471.
[30] A. Fujimori *et al.*, Phys. Rev. B **46**, 9841 (1992); K. Morikawa *et al.*, *ibid.* **54**, 8446 (1996).